start the numerical solution an initial guess for the state variables is required. The linear profile ($a_1 = 1$, $a_2 = a_3 = a_4 = 0$) is taken together with $\delta\eta = 1$ to be the starting values.

The problem was coded in FORTRAN IV and run on the ICL 1905 E Computer of Cairo University. The values of f, f' and f'' were obtained at the three nodal points. Comparison between values calculated by the present method and those of Ref. 6 is shown in Table 1.

Table 1 Comparison of values of f, f' and f''

η	f		f'		f''	
	Present	Ref. 6	Present	Ref. 6	Present	Ref. 6
1.73	0.47591	0.47597	0.54778	0.54776	0.28897	0.28893
3.46	1.77701	1.77706	0.92169	0.91267	0.10679	0.10678
5.19	3.48062	3.48064	0.99367	0.99565	0.01159	0.01157

The running mill time was about 1.2 sec, compared to 4.3 sec (to get the same accuracy) by using finite difference approach.

Application to Initial Value Problem

Initial value problems can also be dealt with by the present method. Let's consider the equation obtained by the hypersonic small disturbance theory for the perturbed potential flow over a cone in the region between the shock wave and the body surface. The equation reads[7]

$$4f^2f'' - 2ff'^2 = \gamma\omega\frac{f'^{(\gamma+1)}}{\theta^{(\gamma-1)}}(f'' - f'/\theta) \tag{20}$$

where f is the nondimensional stream function, θ is the conical parameter (independent variable), γ is the ratio of specific heats, and ω is a known function of γ and K_s (where K_s is the shock wave hypersonic similarity parameter).[7]

In Eq. (20) primes denote differentiations with respect to θ. Equation (20) is to be solved subject to the initial conditions

$$f(1) = \tfrac{1}{2} \quad \text{and} \quad f'(1) = (\gamma+1)K_s^2/[2+(\gamma-1)K_s^2] \tag{21}$$

The solution starts from the shock wave ($\theta = 1$) and proceeds till f goes to zero (the cone surface). Making use of the linear interpolations

$$f''(\theta) = [f'(\theta) - f'(\theta-\Delta\theta)]/\Delta\theta \tag{22a}$$

$$f'(\theta) = [f(\theta) - f(\theta-\Delta\theta)]/\Delta\theta \tag{22b}$$

where $\Delta\theta$ is a small internal, whose magnitude depends upon the accuracy required. Denoting

$$x_1 = f(\theta); \quad \bar{x}_1 = f(\theta-\Delta\theta)$$

$$x_2 = f'(\theta); \quad \bar{x}_2 = f'(\theta-\Delta\theta)$$

Equations (20) and (22b) thus become

$$\phi_1 = 4x_1^2(x_2 - \bar{x}_2) - 2\Delta\theta x_1 x_2^2 - \frac{\gamma\omega}{\theta^{(\gamma-1)}}x_2^{(\gamma+1)} \times \left(x_2 - \bar{x}_2 - -\frac{\Delta\theta}{\theta}x_2\right)$$

$$\phi_2 = x_1 - \bar{x}_1 - \Delta\theta x_2 \tag{23}$$

subject to the initial conditions given by Eq. (21), where $x_1^0 \equiv f(1) = \frac{1}{2}$ and $x_2^0 \equiv f'(1)$.

The preceding system of equations has been solved by the present method. Taking $\Delta\theta = 0.02$, the running mill time on the ICL 1905 E Computer of Cairo University (for $K_s = 1.58$) is 0.1 sec, compared to 0.25 sec by using the Runge-Kutta scheme. The obtained value of the pressure coefficient (which is a function of f') is the same as in Ref. 7.

References

[1] Bellman, R., "Perturbation Techniques n Mathematics, Physics, and Engineering," Holt, Rinehart and Winston, New York, 1964.

[2] Rasmussen, M. L., "On Hypersonic Flow Past an Unyawed Cones," *AIAA Journal*, Vol. 5, No. 8, Aug. 1967, pp. 1495–1497.

[3] Bellman, R. and Kalaba, R., "Quasilinearization and Non-Linear Boundary Value Problems," Elsevier, New York, 1965.

[4] Libby, P. A. and Liu, T. M., "Some Similar Laminar Flows Obtained by Quasilinearization," *AIAA Journal*, Vol. 6, No. 8, Aug. 1968, pp. 1541–1548.

[5] Lew, H. G., "Method of Accelerated Successive Replacement Applied to Boundary Value Equations," *AIAA Journal*, Vol. 6, No. 5, May 1968, pp. 929–931.

[6] Pai, S. I., "Viscous Flow Theory," Vol. 1, *Laminar Flow*, Van Nostrand, New York, 1956.

[7] Van Dyke, M. D., "A Study of Hypersonic Small Disturbance Theory," TN-3173, May 1954, NACA.

A Correlation of Freejet Data

RICHARD T. DRIFTMYER*

Naval Ordnance Laboratory, Silver Spring, Md.

Introduction

THE subject for discussion is the two-dimensional, underexpanded, freejet flowing into a static medium. Interest in freejet studies has been prompted by modeling studies of interacting jet controls.[1] These studies have determined that the interacting jet shock height scales the two-dimensional jet interaction flowfield, and further, a direct correspondence exists between freejet shock heights and those interaction jets.[1] An earlier correlation study of freejet shock heights[2] was based upon axisymmetric nozzle data, both sonic and supersonic, and upon two-dimensional sonic nozzle data. Since then, data which include the supersonic slot nozzle case have been obtained. These results modify the earlier reported correlation. Several graphical solutions by the method of characteristics are also reported.

Experimental Conditions

The experimental apparatus included a slot nozzle mounted transversely between two glass-ported side plates. This assembly was placed in the test section of the wind tunnel which served as a convenient, low-pressure, test cell. The wind-tunnel vacuum pumping plant was used to maintain a constant reservoir pressure, P_b, (surrounding the jet plume). Test conditions and photographs were recorded for jet strengths, P_{0j}/P_∞, ranging from 29.4 to 915.6. Two supersonic jet nozzles were tested with Mach numbers of 2.89 and 2.99 and throat widths of 0.0335 in. and 0.0204 in. respectively. Three sonic jet nozzles of various slot widths were also tested as a check on previously published results.[2]

Experimental Results

An entirely unexpected experimental result was the observed absence of the centerline normal shock wave for the supersonic jet case. Figures 1a, 1b, and 1c show typical photographs of the supersonic jet shock structure. Additional photographic data are found in Ref. 3. Figure 1d shows a typical graphical solution by the method of characteristics. The observed differences between sonic and supersonic freejet plume shapes are shown sketched in Fig. 2a. Embedded within the jet plume are inter-

Received December 29, 1971; revision received March 27, 1972. The research was sponsored by the Naval Air Systems Command (AIR 320).

Index category: Jets, Wakes, and Viscid-Inviscid Flow Interactions.

* Aerospace Engineer, Applied Aerodynamics Division. Member AIAA.

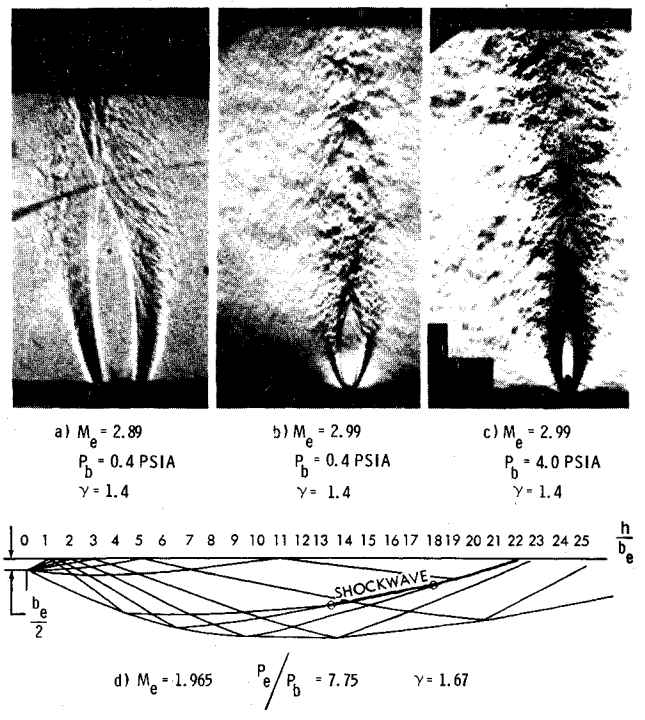

Fig. 1 Two-dimensional jet (slot) plume structure, experimental and graphical.

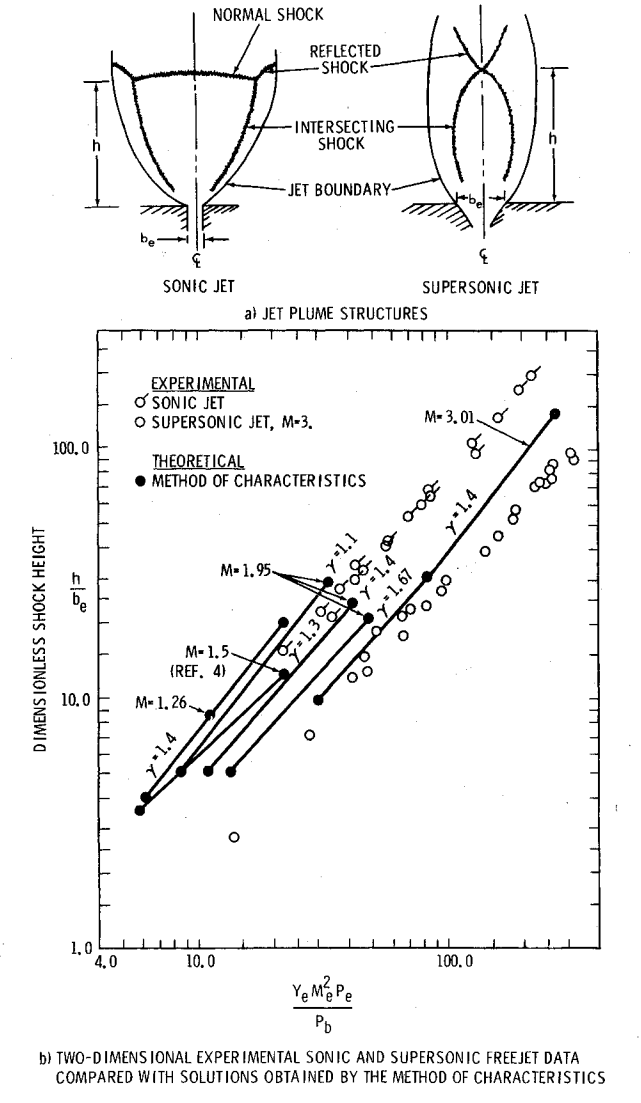

b) TWO-DIMENSIONAL EXPERIMENTAL SONIC AND SUPERSONIC FREEJET DATA COMPARED WITH SOLUTIONS OBTAINED BY THE METHOD OF CHARACTERISTICS

Fig. 2 Experimental and graphical results.

secting and reflected shocks. The normal shock was observed only for the sonic case.

Traditionally, the definition of jet-scale length has been the standoff distance of the normal shock, measured from the nozzle exit plane. The absence of a normal shock in the supersonic case made it necessary to select a characteristic length common to both cases. The intersecting-reflecting shock juncture detachment distance was selected as this length. This new definition agrees closely with the previously used definition since the distance attributed to the curvature of the normal shock made up only a small fraction of the total jet-shock height.

In Fig. 2b the experimental results are shown by the open symbols. The sonic nozzle data has been flagged to distinguish it from the supersonic nozzle data. Data correlation is accomplished following the method of Werle et al.[2] It is simply a cross-plotting of the dimensionless shock height, h/b_e, with the dimensionless back pressure $\gamma_e M_e^2 P_e/P_b$. Note that the 45° slope of the plotted data indicates a linear variation between the dimensionless variables. The sonic freejet data plot matched previous work, however, a definite Mach number shift occurred when the supersonic data was plotted. This shift was at variance with the universal correlation of Ref. 2. As a consequence, this shift was investigated theoretically.

Theoretical Analysis and Results

The theoretical approach used graphical solutions obtained by the method of characteristics (Fig. 1d) with the following restrictions imposed: a) the supersonic jet exits from the nozzle parallel with the jet centerline, b) the jet boundary does not mix with the surrounding static gas, c) the point in the flowfield

SYMBOL	TYPE OF DATA	b_e INCH	M_e	γ_e	P_b PSIA	PROCEDURE	REFERENCE
△	2-D	.0853	2.99	1.4	.36 to .40	EXPERIMENTAL	PRESENT
○					.53 to .59		
0					3.51 to 3.68		
◇		.1271	2.89		.39 to .50		
□		.0157	1.0		.35 to .40		
◇		.0299			.14 to .80		
○		.0599			.09 to .45		
▲		—	1.2565		—		
◣		—	1.9503	1.1	—	METHOD	
◆		—	1.954	1.4	—	OF	
■		—	1.965	1.67	—	CHARACTERISTICS	
◢		—	3.0126	1.4	—		
◣		—	1.5	1.3	—		3
—	AXISYM	—	1.0 to 2.91	1.3 to 1.67	—	EXPERIMENTAL	2

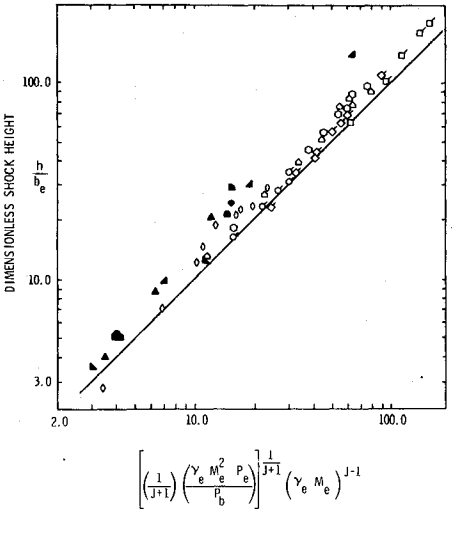

Fig. 3 Universal correlation of freejet data.

where the characteristics of the same family intersect is interpreted as the beginning of the embedded shock wave structure, d) the embedded intersecting shock wave shape in the downstream direction is approximated by the envelope formed from the succeeding intersecting characteristics—extended to the jet centerline. The details of the calculation may be found in Refs. 4 and 5. Assumption d actually causes some overestimation of the freejet height due to the coarse mesh used. This overestimation may also be partially accounted for by the turbulent mixing which actually occurred at the jet boundary interface as seen in Fig. 1.

The theoretical results are plotted as solid symbols in Fig. 2b. Good qualitative support of the experimentally observed Mach number shift is indicated by the theoretical results computed at Mach = 1.26, 1.95, and 3.01 ($\gamma = 1.4$). Based upon this agreement the characteristics solutions were extended to include the effects of specific heat ratio γ on the freejet height. These results, also shown plotted in Fig. 2b, were calculated at Mach = 1.95 for $\gamma = 1.1$, 1.4, and 1.67 and clearly indicate the influence of γ.

Analysis of Results

It was found that all of the data, which is plotted on Fig. 2b, would collapse onto a single curve when expressed in terms of the dimensionless height, h/b_e, and the product of Mach number and pressure ratio, M_eP_e/P_b as opposed to the dimensionless back pressure ratio $\gamma_eM_e^2P_e/P_b$. This has been done on Fig. 3 where the axisymmetric freejet data correlation of Ref. 2 has also been included for completeness. Note that the abscissa in Fig. 3 has been generalized to accomodate both axisymmetric and two-dimensional data. The index number j is understood to be one or zero depending upon whether the jet flow is axisymmetric or two-dimensional, respectively. The final universal curve which results from this correlation of data can be expressed as

$$h/b_e = [1/(j+1)](\gamma_eM_e^2P_e/P_b)^{1/(j+1)}(\gamma_eM_e)^{j-1} \qquad (1)$$

This new result implies that for the two-dimensional freejet case, the dimensionless jet height is independent of the specific heat ratio γ and is only linearly dependent upon the jet exit Mach number.

The observation that the two-dimensional jet height is independent of γ was previously pointed out by Vinson[6] as a result of his computer solutions. This matter was discussed in Ref. 2. Recently, this same observation has been indirectly verified by Thayer and Corlett[7] in their work with the two-dimensional jet interaction problem. They observed experimentally that the flowfield was "insensitive to changes in the injectant specific heat ratio."

The work of Werle et al.[1] indirectly supports the linear dependence of jet Mach number with jet height. The use of Eq. (1) in the two-dimensional jet interaction model of Ref. (1) correctly predicts a decrease of jet amplification with an increase of jet exit Mach number in contradistinction to the recognized inconsistency previously noted in Ref. (1).

Conclusion

The current results are expressed by Eq. (1). It indicates that the jet height varies linearly with jet Mach number for both the axisymmetric and the two-dimensional flow cases. Further, in Eq. (1) the injectant specific heat ratio varies to the one-half power in the axisymmetric case while in the two-dimensional case the jet height is independent of γ.

References

[1] Werle, M. J., Driftmyer, R. T., and Shaffer, D. G., "Two-Dimensional Jet Interaction with a Mach 4 Mainstream," NOLTR 70-50, May 1, 1970, Naval Ordnance Lab., White Oak, Md.

[2] Werle, M. J., Shaffer, D. G., and Driftmyer, R. T., "On Free-Jet Terminal Shocks," *AIAA Journal*, Vol. 8, No. 12, Dec. 1970, pp. 2295–2297.

[3] Driftmyer, R. T., "The Shock Heights of Static Free Jets," NOLTR 72-23, Jan. 11, 1972, Naval Ordnance Lab., White Oak, Md.

[4] Pack, D. C., "On the Formation of Shock Waves in Supersonic Gas Jets (Two-Dimensional Flow)," *Quarterly Journal of Mechanics and Applied Mathematics*, Vol. 1, Pt. 1, 1948, pp. 1–17.

[5] Shapiro, A. H., "The Dynamics and Thermodynamics of Compressible Fluid Flow," *Method of Characteristics for Two-Dimensional Supersonic Flow*, Vol. 1, Ronald Press, New York, 1953, pp. 462–528.

[6] Vinson, P. W., "Prediction of Reaction Control Effectiveness at Supersonic and Hypersonic Speeds," Rept. OR 6487, March 1965, Research Div. of Martin-Orlando, Orlando, Fla.

[7] Thayer, W. J. and Corlett, R. C., "An Investigation of Gas Dynamic and Transport Phenomena in Two-Dimensional Jet Interaction Flow Field," AIAA Paper 71-561, Palo Alto, Calif., 1971.

Boundary-Layer Effects on Pressure Variations in Ludwieg Tubes

ECKART PILTZ*
Technische Hochschule Darmstadt, Germany

Nomenclature

a = speed of sound
d = inner diameter of storage tube
L = length of storage tube
M = Mach number
p = (static) pressure
p_S = stagnation pressure
r = inner radius of storage tube
Re_d = Reynolds number (formed with d)
t = time
δ_N = boundary-layer thickness at nozzle inlet
ν_{00} = kinematic viscosity at room temperature and atmospheric pressure
Δ = signifies difference

Subscripts
0 = initial (storage) state
1 = state in ideal flow behind expansion fan
at = atmospheric

Introduction

LUDWIEG Tubes are rather simple gasdynamic testing facilities in which almost steady sub- and supersonic flow can be maintained for some period of time. Basic to the operation cycle of a Ludwieg Tube is an expansion wave which propagates down a cylindrical tube serving as gas storage. The difference between the real and the ideal behavior of the flow behind the expansion wave is caused by the finite viscosity and conductivity of the operating gas, usually air.

After the head of the expansion wave has passed some point of the storage tube a boundary layer develops at the tube wall by which mass is being transported from the near-wall region into the remaining potential core of the flow. When the boundary layer has grown together tube flow is assumed. In both cases waves are created travelling up- and downstream through the tube and changing the fluid-mechanical and thermodynamic state of the gas. Especially the flow ahead of the nozzle is accelerated by these waves. As the boundary condition $M = 1$ in the throat of the nozzle will be maintained in quasistationary flow part of the oncoming waves will be reflected. Only the net effect of these concurring wave systems can be measured at any particular point in the storage tube. The boundary-layer growth and the resulting variations of pressure and stagnation pressure were calculated in the theory[1] by E. Becker.

Received January 10, 1972; revision received April 4, 1972.
Index categories: Boundary Layer and Convective Heat Transfer—Turbulent; Nozzle and Channel Flow.

* Scientist, Technische Stroemungslehre.